Context-dependent consequences of lagged effects in demographic models

Eric R. Scott[1], María Uriarte[1], Emilio M. Bruna[1]

[1]Department of Wildlife Ecology and Conservation, University of Florida, Gainesville, Florida 32611-0430 USA

[2]Department of Ecology, Evolution and Environmental Biology, Columbia University 1200 Amsterdam Avenue, New York, New York 10027 USA

[3]Center for Latin American Studies, University of Florida, Gainesville, Florida 32611-5530 USA

[4]Biological Dynamics of Forest Fragments Project, INPA-PDBFF, CP 478, Manaus, Amazonas 69011-970 Brazil

(draft: 2 September 2025)

Abstract

Text of 150 words max summarizing this amazing paper.

Keywords: demography, environmental stochasticity, integral projection models, lagged effects, structured population models, population dynamics

Manuscript elements: Figures 1-4, Tables 1-6

Manuscript type: e-note

Introduction

Current environmental conditions can have large and immediate effects on the growth, survival, or reproduction of long-lived organisms. There is also mounting evidence, however, for intervals that range from months to years between environmental conditions and the resulting changes in demographic vital rates. These *Lagged Effects*, also known as *Delayed Life-history Events* (i.e., DLHEs) (Beckerman et al. 2002), can simultaneously affect an entire cohort (e.g., juveniles hatching during a period of scarcity will all have delayed maturation and lower lifetime fecundity) or only a subset of the population (e.g., cold temperatures in one year lead to reduced flowering by potentially reproductive individuals in the next). In addition, the temporal delay between an environmental event and changes in demographic vital rates depends on both the intensity of the event and its timing relative to the underlying physiological processes (Criley and Lekawatana 1994; Evers et al. 2021). A drought during the early stages of gestation or floral bud formation, for example, might have a much larger impact on the number of fruits or offspring produced than one at a later stage of the reproductive process. The delay or intensity of lagged effects can also be location- or habitat-specific, with individuals in some sites or habitats buffered against – or able to recover more quickly from - the delayed effects of environmental variation.

Because Lagged Effects are often directly linked to reproduction and survival, it has been argued they could have major but underappreciated consequences for population dynamics (Beckerman et al. 2002). While recent studies suggest this could indeed the case (Williams et al. 2015; e.g., Molowny-Horas et al. 2017; Tenhumberg et al. 2018), broader efforts to test this hypothesis have face a number of obstacles (Metcalf et al. 2015). Empirical tests of putative lagged effects because these are challenging to design, implement, and maintain (Kuss et al. 2008). While one could use conceivably use observational data to detect lagged effects, doing so requires long-term data on both the putative lagged effect (e.g., reduced probability of flowering) and its potential

environmental drivers (e.g., drought during early floral development), and such coupled data sets are rare (sensu Evers et al. 2021). In addition, the methods for both identifying lagged effects and modeling their demographic impacts can be challenging to implement. For example, many of the potentially applicable statistical methods have stringent assumptions and data requirements rarely met by ecological data (Metcalf et al. 2015), while the including complex biological processes in demographic models can render them less tractable or amenable to analysis using currently available tools. Addressing these challenges is a major undertaking; the value of doing so will depend on the effort required vs. the potential consequences of failing to consider lagged effects - consequences that range from overestimating projections of population growth rate (i.e., λ) in a conservation setting to drawing invalid conclusions regarding support for the predictions of ecological or evolutionary theory.

Integral Projection Models (i.e., IPMs) are an important and widely used tool for studying demography and population dynamics (Ellner and Rees 2006; Rees and Ellner 2009; Rees et al. 2014). Their flexibility, in concert with a rapidly growing suite of software, data, and other resources (Salguero-Gómez et al. 2015; Ellner et al. 2016; Levin et al. 2021), have facilitated their use to study a wide range of topics in ecology, evolution, and conservation Crone et al. (2011). Mathematical and statistical advances (e.g., Williams et al. 2012; Brooks et al. 2019) have rapidly expand the scope of questions and biological processes that can be investigated with these models (e.g., Metcalf et al. 2015; Ellner et al. 2016; Rees and Ellner 2016). Here we investigate how including lagged effects in Integral Projection Models influences projections of λ and population structure.

We have previously shown that the effects of precipitation extremes on the demographic vital rates of an Amazonian understory herb (*Heliconia acuminata*, Heliconiaceae) can be delayed up to 36 months (Scott et al. 2022), with the presence and duration of these lagged effects varying by vital rate and habitat. We parameterized three classes of Integral Projection Models - a deterministic IPM, a stochastic IPM, and a

stochastic IPM with lagged effects of precipitation on vital rates - for populations in two habitat type (i.e., continuous forest vs. forest fragments). Based on previous studies (Bruna and Kress 2002; Bruna 2003; Bruna and Oli 2005) and demographic theory (Tuljapurkar 1990; Caswell 2001) we predicted that: (i) projections of λ from deterministic models would be higher than those of stochastic models, and that (ii) λ is lower for Forest Fragment than Continuous Forest populations regardless of model, but the difference between the two habitats is greatest for the IPM with lagged effects.

Methods

Study System and Demographic Data

Heliconia acuminata (Heliconiaceae) is a perennial, self-incompatible monocot that is distributed throughout much of the Amazon basin (Kress 1990). While some *Heliconia* species grow in large aggregations on roadsides, gaps, and in other disturbed habitats, others - including *H. acuminata* - grow primarily in the forest understory (Kress 1983; Ribeiro et al. 2010). Understory *Heliconia* species produce fewer flowers and are pollinated by traplining hummingbirds (Stouffer and Bierregaard 1996; Bruna et al. 2004). The models and analyses here are based on 11 years (1998-2009) of demographic data collected on >8500 *H. acuminata* found at Brazil's Biological Dynamics of Forest Fragments Project (BDFFP), located ~70 km north of Manaus, Brazil. The BDFFP reserves include both continuous forest and forest fragments that range in size from 1-100 ha. These fragment reserves were originally isolated in the early 1980's by the creation of cattle pastures, with the secondary growth surrounding them periodically cleared to ensure their continued isolation. The habitat in all sites is non-flooded lowland rain forest with rugged topography. A complete summary of the BDFFP and its history can be found in Bierregaard et al. (2001).

A complete description of our demographic methods, data, and analyses to date can be

found in Bruna et al. (2023). Briefly, in 1997–1998 a series of 5000 m^2 plots were established in the BDFFP reserves: N=6 in Continuous Forest and N=4 in 1-ha Forest Fragments (i.e., CF and FF, respectively). All of the *Heliconia acuminata* in these plots were marked and measured; the plots were censused annually, at which time a team recorded the size of surviving individuals, marked and measured new seedlings, and identified any previously marked plants that died. Each plot was also surveyed 4-5 times during the flowering season to identify reproductive plants. These surveys were complemented by data on the number of fruits per flowering plant (Bruna 2021) and seeds per fruit (Bruna 2014) that were collected outside of the demographic plots to avoid altering within-plot recruitment. We also conducted experiments to quantify the probability of seed germination and seedling establishment in both forest fragments and continuous forest (Bruna 1999, 2002).

Heliconia acuminata in our site begin flowering early in the rainy season (e.g., January) and most reproductive plants produce a single infloresence (range = 1–7) with 20–25 flowers (Bruna and Kress 2002). Fruits mature April-May and have 1–3 seeds per fruit ($\bar{x} = 2$) that are dispersed by a thrush and several species of manakin (Uriarte et al. 2011). Dispersed seeds germinate approximately 6 months after dispersal at the onset of the subsequent rainy season, with rates of germination and seedling establishment higher in continuous forest than forest fragments (Bruna 1999, 2002). On average plots in CF also had more than twice as many plants as the plots in 1-ha fragments (CF median = 788, range = (201-1549); 1-ha median = 339, range = (297-400)).

Construction of Integral Projection Models

We projected the growth rate and structure of *Heliconia acuminata* with three classes of IPMs - Deterministic, Stochastic, and Stochastic with Lagged Environmental Effects. Each of these IPMs required different functional forms of the underlying vital rate functions used to describe the *H. acuminata* life cycle (Figure 1). All models were density-independent,

with the deterministic model serving as the foundation for the more complex models. Our modeling workflows were managed using the `targets` R package (Landau 2021); in adddition to ensuring reproducibility this allowed us to track computational time spent processing and analyzing each class of IPM.

(1) Deterministic IPM: In this model the size and structure of a population in year $t+1$ is determined by the survival and growth of plants alive in year t (Equation 1) plus the number of new seedlings that entered the population (Equation 2).

$$n(z', t+1) = R(z')n_s(t) + \int_L^U P(z', z)n(z, t)\, dz \tag{1}$$

$$n_s(t+1) = \int_L^U F(z)n(z, t)\, dz \tag{2}$$

Equation 1 has two components. The first is the sub-kernel $P(z', z)$, which describes the size-dependent survival and growth/regression of mature plants (Equation 3):

$$P(z', z) = s(z)G(z', z) \tag{3}$$

The second is sub-kernel $R(z')$, which describes the survival of seedlings established in year t and their size when entering the mature plant population in year $t+1$ (Equation 4):

$$R(z') = s_s G_s(z') \tag{4}$$

Note that in Equation 4 both the probability that new seedlings survive their first year, s_s, and their size at the end of this year, $G(z', z)$, are size-independent. IPMs can include transitions between individuals from a discrete state to a continuous one (i.e., from 'seedling' to 'mature plant of size z',' Ellner et al. 2016); we treat seedlings as a distinct and discrete category because they have lower survival and growth in their first year than comparably sized plants (Bruna 2003; Scott et al. 2022).

The number of new seedlings entering the population in year $t+1$ is a function of the number of mature plants in year t and a sub-kernel describing the size-dependent fecundity of these individuals (Equation 5):

$$F(z) = p_f(z)f(z)g \tag{5}$$

Both the probability that a mature plant will flower, $p_f(z)$, and the number of seeds a flowering plant will produce, $f(z)$, are size-dependent. All seeds germinate and establish as seedlings with probability g.

We used the annual census data (Bruna 2003) to fit the deterministic vital rate functions for growth, survival, and flowering in each habitat type (i.e., Fragments, Continuous Forest; the data from all plots within a habitat class were pooled to create a single 'summary population' for the CF and FF habitats (Bruna 2003). For established plants these were modeled as a smooth function of size in the previous census with generalized additive models (GAMs) fit with the `mgcv` library (Wood 2011) for the R statistical programming language (R Core Team 2020). For consistency, seedling survival and growth were also modeled using GAMs, but without size in the previous census as a predictor (i.e. 'intercept-only' models). For growth models a scaled t family distribution provided a better fit to the data than a Gaussian fit, as the residuals with a simple Gaussian model were Leptokurtic. To model size-specific fecundity we used the data on fruits per flowering plant (Bruna 2021), seeds per fruit (Bruna 2014), and the experimentally-derived estimates of seed germination and seedling establishment (Bruna 1999, 2002).

(2) Stochastic IPMs: To include temporal stochasticity in our IPMs we included a random effect of year. This was done using a factor–smooth interaction that allowed the functional form of the relationship between plant size and vital rates to vary among transition years (Figure 1). We generated kernels for every transition year using the

long-term survey data (Bruna et al. 2023) and random smooths for year. We then randomly selected one of these sets of kernels to use in each iteration of the IPM. This procedure is equivalent to *'kernel resampling'* (*sensu* Metcalf et al. 2015) or matrix selection for matrix population models (Caswell 2001).

(3) Stochastic IPMs with lagged effects of precipitation on vital rates: We explicit modeled the lagged effects of precipitation extremes on vital rates using the procedure described in Scott et al. (2022). Briefly, we first calculated the Standardized Precipitation Evapotranspiraton Index (i.e., SPEI) for our study site using a published gridded dataset based on ground measurements (Xavier et al. 2016). After we fit vital rate models using the long-term survey data (Figure 1), we modeled delayed effects of SPEI with Distributed Lag Non-linear Models (i.e., DLNMs) with a maximum lag of 36 months (Scott et al. 2022). To iterate these parameter-resampled IPMs (*sensu* Metcalf et al. 2015) we first created a random sequence of SPEI values by sampling years of the observed (monthly) SPEI data. For every year we then calculated a lag of 36 months from the month in which that year's census was completed. These values were then used to predict the fitted values from vital rate models, which generated different kernels for each iteration of the IPM. Though the kernels of successive iterations are not entirely independent – the SPEI values used to calculate vital rates include values used in the previous two iterations – they are ergodic.

All IPMs were constructed and iterated using the `ipmr` package (Levin et al. 2021) for the R statistical programming language (R Core Team 2020). The IPMs used 100 meshpoints and the midpoint rule for calculating kernels. For each type of IPM we iterated the model for 1000 time steps, but discarded the first 100 time steps to omit transient effects. Stochastic growth rates (λ_s) were calculated as the average $ln(\lambda)$ from each time step (Caswell 2001) and then back-transformed to allow for direct comparison with projections of λ from deterministic models. The initial starting vector primarily influences a population's transient dynamics; we therefore used the distribution of established plant

sizes and proportion of seedlings in the full demographic data set as the initial population vector for all models.

Finally, We estimated the 95% confidence intervals for each IPMs projections of λ. To do so we first created 500 populations for each habitat type by sampling individual plants with replacement (i.e., bootstrapping) until the population size of each matched that of the initial population vector. We then re-fit the vital rate models for growth, survival, and flowering for each of these bootstrapped population and constructed new IPMs for each population as above (the models for germination and establishment rate, fruits per flowering plant, and seeds per fruit were not refit because these were estimated using different data sets). The projections of λ for the new populations were then used to estimate the upper and lower 95% bias-corrected percentile intervals (Caswell 2001; Manly 2018).

Statistical analyses

Comparison of λ in Continuous Forest and Forest Fragments. To determine if the deterministic projections of λ for Continuous Forest and Forest Fragment populations were significantly different we used the randomization test procedure described by Caswell (2001). Briefly, we randomly assigned plants with their demographic history among two populations, R_1 and R_2, that were equal in size to the original CF and FF populations. We then calculated λ^{R_1}, λ^{R_2}, and the absolute value of the difference between the two (i.e., θ). This was repeated N = 1000 times, after which we determined the proportion of simulations in which θ was greater than the observed difference between λ^{CF} and λ^{FF} (i.e., $P[\theta \geq \theta_{obs}]$).

We used a Generalized Linear Model to compare the projections of λ from the two stochastic IPMs. We modelled the lambda as a function of IPM type (kernel-resampling vs parameter-resampling) and Habitat (continuous forest vs. fragments), and the interaction of IPM type and Habitat. Because the response variable (λ) was continuous we used the

Gaussian distribution with the identity function in our model. We verified the model assumptions by plotting residuals versus fitted values.

Population Structure. Finally, we compared the structure of populations through the first 250 time steps in each habitat by each of the stochastic IPMs (i.e, kernel- vs. parameter-resampling). At each time step, we assigned the individuals to one of four stage classes based on plant size, probability of survival, and probability of reproduction (see Table Table 3). We then calculated the proportion of the population that was in each stage class in each habitat for each IPM type. Comparing the means and variances of these proportions will allow us to determine (1) if the two IPMs project different population structures over time, (2) if the population structure for a given IPM is consistent across habitat type. Because Shapiro-Wilk tests indicated that the distributions of proportions were not normally distributed, we used the non-parametric Ansari-Bradley Test to compare the distribution of proportions in each habitat x stage combination. These analyses were conducted using the R libraries `rstatix` and `vartest`, respectively (Kassambara 2023; Cosar and Dag 2024).

Results & Discussion

All IPMs projected higher population growth rates for *Heliconia acuminata* populations in Continuous Forest than for those in Forest Fragments (Table 2, Table 6). The differences between λ^{CF} and λ^{FF}, which ranged from 1.19-2%, were significant for both deterministic ($P[\theta \geq \theta_{obs}] = 0$, N = 1000 randomization) and stochastic IPMs (Table 6). There were also significant effects of IPM Type, Habitat, and their interaction on λ (Table 6). Deterministic λ was nearly identical to the average λ from kernel-resampled IPMs (Figure 3), which is somewhat surpring given that stochasticity is predicted to reduce population growth rates (Tuljapurkar et al. 2003; Doak et al. 2005; Metcalf et al. 2015). However including lagged effects in IPMs resulted in projections of λ that were on average 1.5-2% lower than those of

deterministic models, with 70-76% of projections below deterministic λ (Figure 3). The IPMs with lagged effects also appear to be more accurate - the underlying vital rate models for IPMs with lagged effects all had the best fit to the survey data (dAIC = 0, Table 1).

Including lagged effects in IPMs also resulted in significantly less predictable projections of population structure, both within (Figure 2 a) and across habitats (Figure 2 b, Table 4). This variability is particularly notable in forest fragments (Figure 4, Table 5), where we have previously shown lagged effects have very large impacts on growth and survival (Scott et al. 2022). The deterministic IPM for Continuous Forest projected slightly more of the smallest and largest plants than the one for Forest Fragments. In other words, populations in forest fragments had proportionately less recruitment and fewer individuals growing into the larger, reproductive size classes (Bruna and Oli 2005). This shift towards intermediately sized, pre-reproductive plants in forest fragments is even more dramatic when using the parameter-resampled stochastic IPM (Figure 2 b).

What are the implications of these results for the use of IPMs to study plant demography? First, they suggest that failing to include lagged effects in models could result in underestimates of λ. While relative differences in λ may be sufficient for some tests of theory, they may be critical in conservation or management settings because even small differences in λ can have major consequences for population dynamics. They could also be critical for studies assessing the effects of climate change, given many DLHE are climate driven. That said, there is a cost to including lagged effects in models, even in if they are more accurate. While Deterministic and Kernel-resampled Stochastic IPMs took only ~0.02 and ~0.07 min to iterate (respectively), the Stochastic IPMs with using parameter-resampled kernels and lagged effects took ~87.12 min. This is largely due to the required computational resources and algorithms (i.e., `predict()`), which are much slower forGeneral Additive Models (i.e., GAMs) with 2D smooths because of the much higher number of knots than for the GAMs used in Determinsitic and Kernel-resampled IPMs. Advances in computational power and access to high-performance computing resources

could lower this cost.

Computational power cannot compensate for limited data, however. Detecting lagged effects and evaluating their consequences requires long-term demographic data - data that are only available for a relatively small number of species, few of which are in the tropics. The increasing evidence that lagged effects are ubiquitous, and that they can have major demographic impacts, underscores the need to support the collection of such long-term data, the complementary development of experimental and statistical approaches to disentangling lagged effects, and community driven efforts to identify priority or model systems for in-depth investigation.

Acknowledgments

We thank _____, _____, and _____ anonymous reviewers for helpful discussions and comments on the manuscript. We also thank Sam Levin for his help with the `ipmr` package. Financial support for collecting the demographic data used in this study was provided by the U.S. National Science Foundation (awards INT 98-06351, DEB-0309819, DEB-0614149,DEB-0614339, and DEB-1948607). This article is publication no. _____ in the BDFFP Technical series. The authors declare no conflicts of interest.

CRediT Statement

ERS contributed to the conceptualization, methodology, formal analysis, and led the writing of the original draft. EMB contributed to the conceptualization, methodology, writing, and, acquired funding.

Data Availability Statement

Data and R code used in this study are archived with Zenodo at *(doi and url to be added on acceptance)*.

Literature Cited

Beckerman, A., T. G. Benton, E. Ranta, V. Kaitala, and P. Lundberg. 2002. Population dynamic consequences of delayed life-history effects. Trends in Ecology & Evolution 17:263–269.

Bierregaard, R. O., C. Gascon, T. E. Lovejoy, and R. Mesquita, eds. 2001. Lessons from Amazonia: The ecology and conservation of a fragmented forest. Yale University Press, New Haven.

Brooks, M. E., K. Kristensen, M. R. Darrigo, P. Rubim, M. Uriarte, E. Bruna, and B. M. Bolker. 2019. Statistical modeling of patterns in annual reproductive rates. Ecology 100.

Bruna, E. M. 1999. Seed germination in rainforest fragments. Nature 402:139.

———. 2002. Effects of forest fragmentation on *Heliconia acuminata* seedling recruitment in central Amazonia. Oecologia 132:235–243.

Bruna, E. M. 2003. Are plant populations in fragmented habitats recruitment limited? Tests with an Amazonian herb. Ecology 84:932–947.

———. 2014. Dataset: <Span class="nocase">*Heliconia acuminata* seed set (seeds per fruit). Figshare doi: 10.6084/m9.figshare.1273926.v2.

———. 2021. Dataset: Leaf number, leaf area, shoot number, and height of reproductive H. acuminata. Zenodo https://doi.org/10.5281/zenodo.5041931.

Bruna, E. M., and W. J. Kress. 2002. Habitat fragmentation and the demographic structure of an Amazonian understory herb (*Heliconia acuminata*). Conservation Biology 16:1256–1266.

Bruna, E. M., W. J. Kress, F. Marques, and O. F. da Silva. 2004. *Heliconia acuminata* reproductive success is independent of local floral density. Acta Amazonica 34:467–471.

Bruna, E. M., and M. K. Oli. 2005. Demographic Effects of Habitat Fragmentation on a Tropical Herb: Life-Table Response Experiments. Ecology 86:1816–1824.

Bruna, E. M., M. Uriarte, M. R. Darrigo, P. Rubim, C. F. Jurinitz, E. R. Scott, O. Ferreira da Silva, et al. 2023. Demography of the understory herb Heliconia acuminata (Heliconiaceae) in an experimentally fragmented tropical landscape. Ecology 104:e4174.

Caswell, H. 2001. Matrix population models: Construction, analysis, and interpretation. Sinauer Associates, Sunderland.

Cosar, G., and O. Dag. 2024. *Vartest: Tests for variance homogeneity* (manual).

Criley, R., and S. Lekawatana. 1994. Year around production with high yields may be a possibility for *Heliconia chartacea*. Acta Horticulturae, New ornamental crops and the market for floricultural products 397:95–102.

Crone, E. E., E. S. Menges, M. M. Ellis, T. Bell, P. Bierzychudek, J. Ehrlen, T. N. Kaye, et al. 2011. How do plant ecologists use matrix population models? Ecology Letters 14:1–8.

Doak, D. F., W. F. Morris, C. Pfister, B. E. Kendall, and E. M. Bruna. 2005. Correctly

Estimating How Environmental Stochasticity Influences Fitness and Population Growth. The American Naturalist 166:E14–E21.

Ellner, S. P., D. Z. Childs, and M. Rees. 2016. Data-driven modelling of structured populations: A practical guide to the integral projection model. Springer Science+Business Media, New York, NY.

Ellner, S. P., and M. Rees. 2006. Integral projection models for species with complex demography. American Naturalist 167:410–428.

Evers, S. M., T. M. Knight, D. W. Inouye, T. E. X. Miller, R. Salguero-Gómez, A. M. Iler, and A. Compagnoni. 2021. Lagged and dormant season climate better predict plant vital rates than climate during the growing season. Global Change Biology 27:1927–1941.

Kassambara, A. 2023. *Rstatix: Pipe-friendly framework for basic statistical tests* (manual).

Kress, J. 1990. The diversity and distribution of *heliconia* (Heliconiaceae) in Brazil. Acta Botanica Brasileira 4:159–167.

Kress, W. J. 1983. Self-incompatibility systems in Central American *heliconia*. Evolution 37:735–744.

Kuss, P., M. Rees, H. H. Ægisdóttir, S. P. Ellner, and J. Stöcklin. 2008. Evolutionary demography of long-lived monocarpic perennials: A time-lagged integral projection model. Journal of Ecology 96:821–832.

Landau, W. M. 2021. The targets R package: A dynamic Make-like function-oriented

pipeline toolkit for reproducibility and high-performance computing 6:2959.

Levin, S. C., D. Z. Childs, A. Compagnoni, S. Evers, T. M. Knight, and R. Salguero-Gómez. 2021. Ipmr: Flexible implementation of Integral Projection Models in R. Methods in Ecology and Evolution 12:1826–1834.

Manly, B. F. 2018. Randomization, bootstrap and Monte Carlo methods in biology. chapman; hall/CRC.

Metcalf, C. J. E., S. P. Ellner, D. Z. Childs, R. Salguero-Gómez, C. Merow, S. M. McMahon, E. Jongejans, et al. 2015. Statistical modelling of annual variation for inference on stochastic population dynamics using Integral Projection Models. Methods in Ecology and Evolution 6:1007–1017.

Molowny-Horas, R., M. L. Suarez, and F. Lloret. 2017. Changes in the natural dynamics of *Nothofagus dombeyi* forests: Population modeling with increasing drought frequencies. Ecosphere 8:1–17.

Morris, W. F., and D. F. Doak. 2002. Quantitative conservation biology: Theory and practice of population viability analysis. Sinauer, Sunderland, MA.

R Core Team. 2020. *R: A language and environment for statistical computing*. Vienna, Austria.

Rees, M., D. Z. Childs, and S. P. Ellner. 2014. Building integral projection models: A user's guide. Journal of Animal Ecology 83:528–545.

Rees, M., and S. P. Ellner. 2009. Integral projection models for populations in temporally varying environments. Ecological Monographs 79:575–594.

———. 2016. Evolving integral projection models: Evolutionary demography meets eco-evolutionary dynamics. Methods in Ecology and Evolution 7:157–170.

Ribeiro, M. B. N., E. M. Bruna, and W. Mantovani. 2010. Influence of post-clearing treatment on the recovery of herbaceous plant communities in Amazonian secondary forests. Restoration Ecology 18:50–58.

Salguero-Gómez, R., O. R. Jones, C. R. Archer, Y. M. Buckley, J. Che-Castaldo, H. Caswell, D. Hodgson, et al. 2015. The COMPADRE Plant Matrix Database: An open online repository for plant demography. (M. Rees, ed.)Journal of Ecology 103:202–218.

Scott, E. R., M. Uriarte, and E. M. Bruna. 2022. Delayed effects of climate on vital rates lead to demographic divergence in Amazonian forest fragments. Global Change Biology 28:463–479.

Stouffer, P. C., and R. O. Bierregaard. 1996. Forest fragmentation and seasonal patterns of hummingbird abundance in Amazonian Brazil. Ararajuba 4:9–14.

Tenhumberg, B., E. E. Crone, S. Ramula, and A. J. Tyre. 2018. Time-lagged effects of weather on plant demography: Drought and *Astragalus scaphoides*. Ecology 99:915–925.

Tuljapurkar, S. 1990. Population Dynamics in Variable Environments. (S. Levin, ed.)Lecture Notes in Biomathematics (Vol. 85). Springer, Berlin, Heidelberg.

386 Tuljapurkar, S., C. C. Horvitz, and J. B. Pascarella. 2003. The Many Growth Rates and
387 Elasticities of Populations in Random Environments. The American Naturalist
388 162:489–502.

389 Uriarte, M., M. Anciães, M. T. B. da Silva, R. Rubim, E. Johnson, and E. M. Bruna. 2011.
390 Disentangling the drivers of reduced long-distance seed dispersal by birds in an
391 experimentally fragmented landscape. Ecology 92:924–937.

392 Williams, J. L., H. Jacquemyn, B. M. Ochocki, R. Brys, T. E. X. Miller, and R. Shefferson.
393 2015. Life history evolution under climate change and its influence on the population
394 dynamics of a long-lived plant. Journal of Ecology 103:798–808.

395 Williams, J. L., T. E. Miller, and S. P. Ellner. 2012. Avoiding unintentional eviction from
396 integral projection models. Ecology 93:2008–2014.

397 Wood, S. N. 2011. Fast stable restricted maximum likelihood and marginal likelihood
398 estimation of semiparametric generalized linear models 73:3–36.

399 Xavier, A. C., C. W. King, and B. R. Scanlon. 2016. Daily gridded meteorological
400 variables in Brazil (1980–2013). International Journal of Climatology 36:2644–2659.

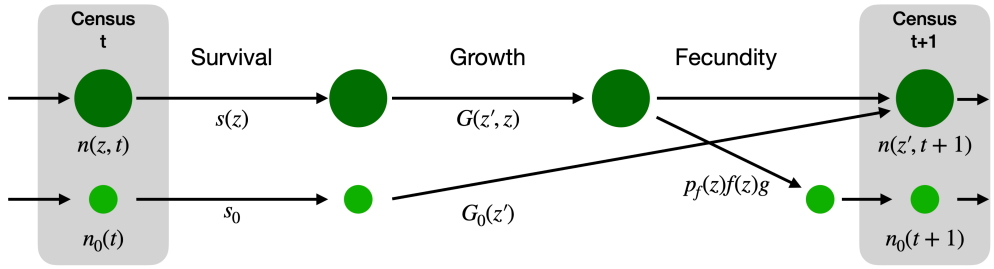

Description	Deterministic	Stochastic, kernel-resampled	Stochastic, parameter-resampled
Survival	$s(z)$	$s_y(z)$	$s(z;\theta_{0-36})$
Growth	$G(z';z)$	$G_y(z';z)$	$G(z',z;\theta_{0-36})$
Flowering	$p_f(z)$	$p_{f_y}(z)$	$p_f(z;\theta_{0-36})$
Size-specific fecundity	$f(z)$	$f(z)$	$f(z)$
Germination & establishment	g	g	g
Seedling survival	s_0	s_{0_y}	$s_0(\theta_{0-36})$
Seedling growth	$G_0(z')$	$G_{0_y}(z')$	$G_0(z';\theta_{0-36})$

fig. 1. Life cycle diagram of *Heliconia acuminata*. Each transition is associated with an equation for a vital rate function. The functions shown on the diagram correspond to those used to construct a general, density-independent, deterministic IPM. The table below shows the equivalent equations for stochastic, kernel-resampled IPMs and stochastic, parameter-resampled IPMs.

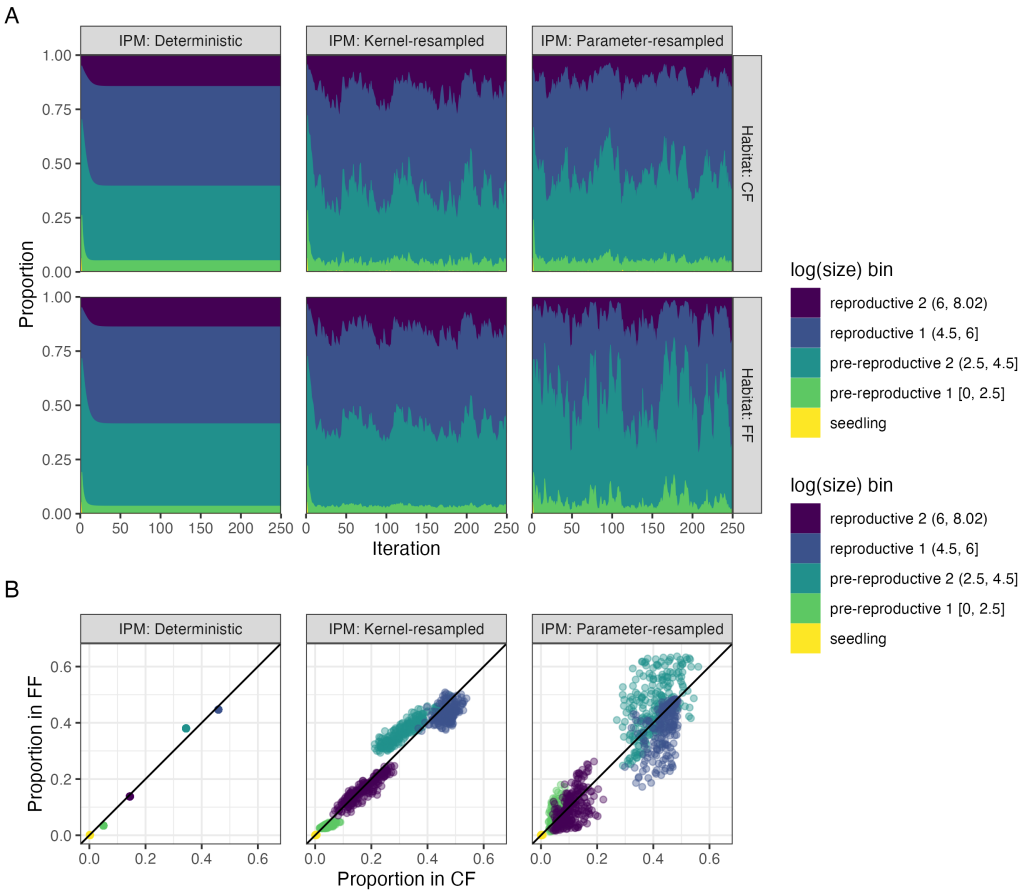

fig. 2. **(A)** The change over time in the the proportion of *Heliconia acuminata* populations in different size/stage classes when simulating population dyammics in Continuous Forest (CF) or Forest Fragment (FF) with three different Integral Projection Models. Results are shown for the first 250 iterations of populations; for the criteria used to define the size categories see Table 3. **(B)** The relative proportion of the population in each size class (FF vs. CF) for 250 iterations of each IPM model. Note that this excludes transient dynamics (iterations 1-30). Values on the 1-1 line indicate an iteration where CF and FF have the same proportion of the population in a given size class.

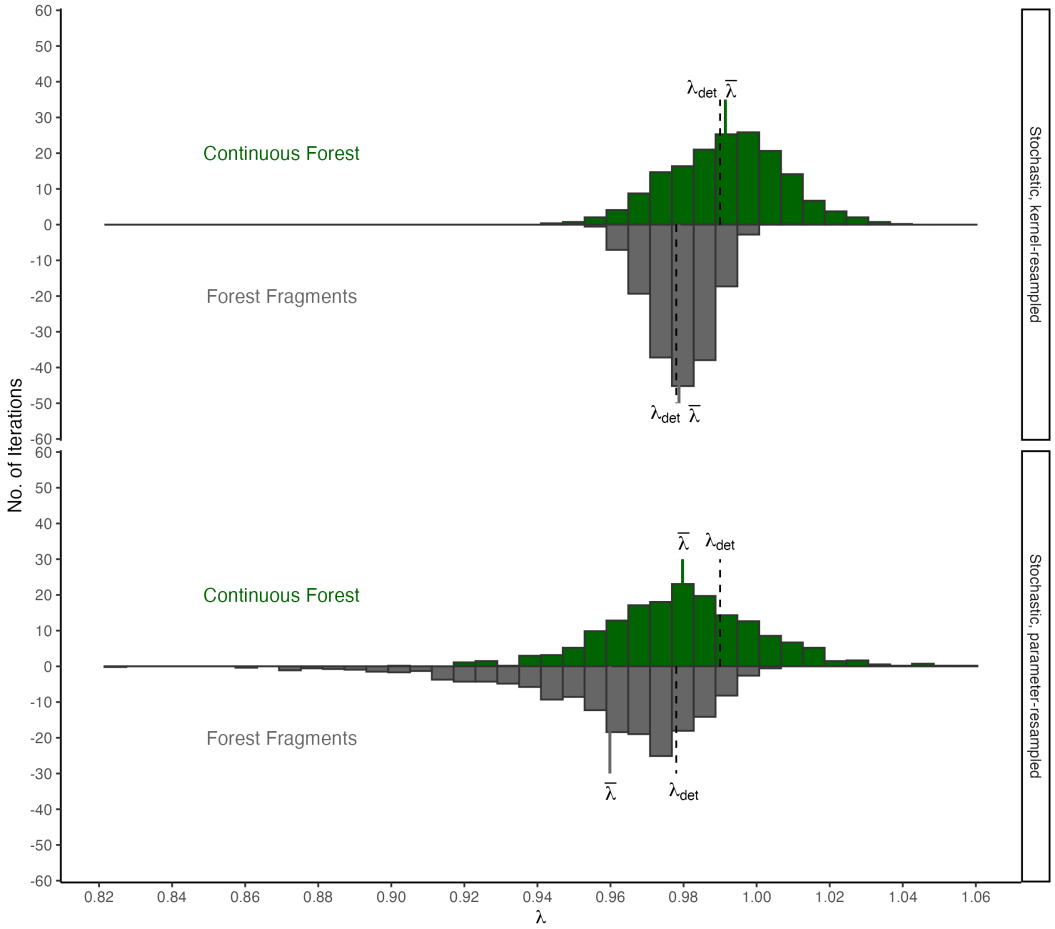

fig. 3. Distribution of 900 values of λ projected with (A) Stochastic, kernel-resampled IPMs and (B) Stochastic, paramenter-resampled IPMs. IPMs were used to project λ for both Continuous Forest (above, in green) and Forest Fragments (below, in gray). The solid line indicates the mean value of λ, the dashed line indicates the value of λ in that habitat projected with Deterministic IPMs.

Table 1: Comparison of vital rate models used to build IPM. The 'Effect of Environment' column describes how environmental effects were included in models. Those with 'none' were used to build deterministic IPMs; those with a random effect of year were used to build stochastic, kernel-resampled IPMs; and those with a distributed lag non-linear model (DLNM) were used to build stochastic, parameter-resampled IPMs. 'edf' is the estimated degrees of freedom of the penalized GAM. ΔAIC is calculated within each habitat and vital rate combination. ΔAIC within 2 indicates models are equivalent.

Habitat	Vital Rate	Effect of Environment	edf	ΔAIC
Continuous Forest				
	Survival	Random effect of year	43.26	0.00
		DLNM	19.72	78.92
		None	4.98	260.01
	Growth	Random effect of year	78.43	0.00
		DLNM	23.87	158.46
		None	7.81	1896.03
	Flowering	DLNM	19.59	0.00
		Random effect of year	17.19	1.63
		None	7.47	381.86
	Seedling survival	None	1.00	0.00
		Random effect of year	1.82	1.39
		DLNM	4.01	1.53
	Seedling growth	Random effect of year	9.47	0.00
		DLNM	8.95	2.90
		None	1.00	172.33
Forest Fragments				
	Survival	DLNM	14.95	0.00
		Random effect of year	19.21	35.68
		None	4.33	51.25
	Growth	DLNM	25.18	0.00
		Random effect of year	37.84	199.98
		None	5.60	382.76
	Flowering	DLNM	20.61	0.00
		Random effect of year	13.81	27.40
		None	5.01	101.70
	Seedling survival	DLNM	5.57	0.00
		Random effect of year	5.09	5.72
		None	1.00	6.49
	Seedling growth	Random effect of year	6.25	0.00
		DLNM	8.18	2.29
		None	1.00	5.74

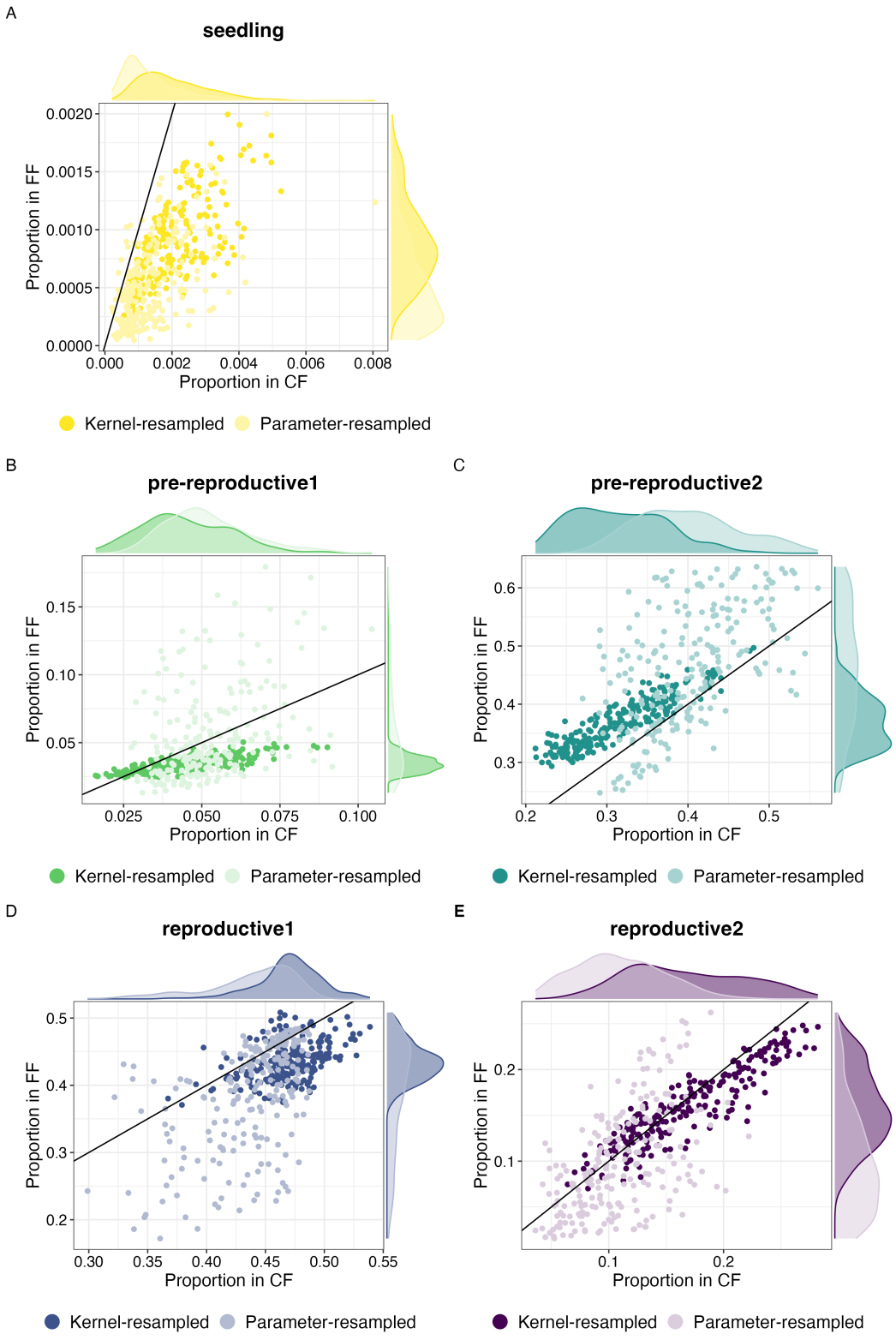

fig. 4. The relative proportion of the population in each size class (FF vs. CF) for each of 250 iterations of the kernel-resampled (dark shading) and parameter-resampled IPM models (light shading). Values on the 1-1 line indicate an iteration where CF and FF have the same proportion of the population in a given size class; the marginal plots indicate the distribution of these relative proportions for each class of IPM in each habitat. Note that both the scatterplots and marginal plots exclude transient dynamics (iterations 1-30).

Table 2: Population growth rates for continuous forest (CF) and forest fragments (FF) under different kinds of IPMs with bootstrapped, bias-corrected, 95% confidence intervals.

IPM	Habitat	λ	(Lower, Upper 95% CI)
Deterministic			
	FF	0.9778	(0.9736, 0.9823)
	CF	0.9897	(0.9877, 0.9920)
Stochastic, kernel resampled			
	FF	0.9787	(0.9735, 0.9835)
	CF	0.9913	(0.9892, 0.9939)
Stochastic, parameter-resampled			
	FF	0.9595	(0.9459, 0.9689)
	CF	0.9795	(0.9752, 0.9867)

Table 3: Size and stage categories used for comparing *Heliconia acuminata* population structure. Note that seedlings are a discrete size class not based on size (see *Methods* for additional details).

Category	Log(size)	Avg. prob. survival	Prob. flowering
Seedlings	-	-	-
Pre-reproductive 1	0–2.5	≤ 0.9	≈ 0
Pre-reproductive 2	2.5-4.5	≥ 0.8	≈ 0
Reproductive 1	4.5-6	≥ 0.95	≤ 0.25
Reproductive 2	≥ 6	≥ 0.95	≥ 0.2

Table 4: Results of statistical tests comparing the variance in the proportion of each habitat's population projected to be in each stage class by kernel-resampled vs. parameter resampled IPMs (N = 220 projections per stage class). The variances for each habitat x stage class x IPM combination can be found in Table 5. Comparisons where the p-value of the test was < 0.05 are indicated with an asterisk.

Stage	Habitat	Statistic	df	p value
Seedling				
	CF	4.59	1	0.032*
	FF	11.51	1	0.001*
Pre-reproductive 1				
	CF	8.73	1	0.003*
	FF	96.13	1	< 0.0001*
Pre-reproductive 2				
	CF	0.99	1	0.319
	FF	39.67	1	< 0.0001*
Reproductive 1				
	CF	0.57	1	0.452
	FF	61.58	1	< 0.0001*
Reproductive 2				
	CF	0.11	1	0.745
	FF	18.78	1	< 0.0001*

Table 5: Summary statistics (median, mean, and variance) describing the proportion of populations projected to be in each of five life-history stages by kernel- and parameter-resampled IPMs (N = 220 projections for each IPM class x habitat combination.)

		Median		Mean		Variance	
Stage	IPM	CF	FF	CF	FF	CF	FF
Seedling							
	Kernel-resampled	0.0018	0.0009	0.0020	0.0020	0.000001	0.000000
	Parameter-resampled	0.0011	0.0004	0.0014	0.0014	0.000001	0.000000
Pre-reproductive 1							
	Kernel-resampled	0.0426	0.0340	0.0450	0.0450	0.000203	0.000034
	Parameter-resampled	0.0499	0.0438	0.0522	0.0522	0.000192	0.001167
Pre-reproductive 2							
	Kernel-resampled	0.3097	0.3677	0.3147	0.3147	0.003354	0.001884
	Parameter-resampled	0.3975	0.4613	0.4002	0.4002	0.003934	0.010380
Reproductive 1							
	Kernel-resampled	0.4725	0.4332	0.4704	0.4704	0.000736	0.000822
	Parameter-resampled	0.4464	0.4049	0.4371	0.4371	0.001481	0.006388
Reproductive 2							
	Kernel-resampled	0.1630	0.1554	0.1679	0.1679	0.002630	0.001745
	Parameter-resampled	0.1062	0.0882	0.1092	0.1092	0.001427	0.003213

Table 6: Estimated parameters, standard errors, t-values and P-values for the GLM of the effect of Habitat and IPM Type on projections of lambda.

Term	Estimate	SE	z value	P value
(Intercept)	0.98	0	1568.20	0
$Habitat_{FF}$	-0.02	0	-22.52	0
IPM_{Stoch}	0.01	0	13.27	0
$Habitat_{FF} : IPM_{Stoch}$	0.01	0	5.76	0